

Method to Balance Thermals for Multi-functional 3D MJF Printing

Aja Hartman, Lihua Zhao
HP Laboratories, 1501 Page Mill Road, Palo Alto, CA, USA

Abstract

HP's Multi Jet Fusion (MJF) is a powder-based additive manufacturing technology that selectively melts polymer powder, in a layer-by-layer fashion to create 3D parts. There are several different voxel properties that can be modulated using MJF including multi-color, ductility, conductivity, among others. Creating mechanically uniform multi-material parts with varying voxel properties throughout is challenging due to the liquid creating a competing cooling and active absorbing components that effect the temperature of printed parts differently. Here, we balance fusibility by utilizing a thermal imaging and an agent loading sweep thermal profile characterization print for each individual agent. We then digitally control the agent loading based on this data set and dynamic thermal imaging to produce a uniform temperature profile. This ensures even fusing throughout multi-agent printed parts, shown by uniform weight measurements of multi-color cubes from average weight 1.4 ± 0.2 g to 1.5 ± 0.1 g.

1. Introduction

Additive manufacturing (AM) is the process of building a part by adding material in successive layers. AM is a key contributor to the industrial revolution, Industry 4.0, which is characterized by the integration of advanced production systems with both automation [1]-and information technologies [2]. 3D printers are an example of these advanced production systems, utilizing data to improve production effectiveness and efficiency through design optimization and process control [3]. AM benefits include increased design complexity, small batch production, and short lead times, which has led to its adoption with the industry estimated to be USD 16.4 billion in 2022 and expected to grow 21.8% in the next forecast period [4]. One of these 3D printing technologies is Multi Jet Fusion (MJF), a powder bed fusion (PBF) archetype.

The MJF print process starts with a computer aided design (CAD) model that is sliced to form a stack of 2-dimensional (2D) images. Then, an adequate warming base is formed from the process of spreading powder and heating using infrared (IR) radiating lamps. The first CAD model 2D geometry slice image is then printed on the powder with an IR absorbing fusing agent (FA) and edges of the geometry defined using detailing agent (DA). The IR fusing lamps pass over the bed, selectively fusing the printed layer. For full fusion to occur in this PBF printing process, the polymer particles must reach above the melt temperature to prevent low density or high porosity parts and decreased mechanical properties [5]. A new layer of powder is spread on top of the previous layer and the process (print, fuse, spread) is repeated until the full object is formed. This printing process describes the basic MJF production system HP Jet Fusion 4200/5200 series. However, MJF technology is not limited to utilizing only FA and DA to form basic 3D geometries, it has the potential to perform in-situ chemistry on a voxel level by selectively jetting functional agents.

Due to the unique nature of MJF microfluidic capability of thermal ink jetting (TIJ) materials, it is possible to deposit a wide array of materials on the voxel level. The current MJF products mainly use FA and DA controlled on the voxel level to determine 3D geometries.

However, other functional agents may include such materials and material properties as silver conductor [6], plasticizer ductility enhancer [7], epoxy stiffener [8], and colorants [9] among others that can change properties of the base polymer. Each of these functional agents has different cooling and IR absorption properties that require fusing, detailing, and functional agent co-modulation to achieve desired properties.

2. Materials and Methods

2.1 Powder material

All experiments were conducted with HP 3D high reusability PA12 powder from HP Inc, Palo Alto, CA USA. PA12 material properties can be found in table 1 [10].

Table 1. HP 3D high reusability PA12 material properties.

| | Value | Method |
|----------------------------|---|------------|
| Powder melting point (DSC) | 187 °C 369 °F | ASTM D3418 |
| Particle size | 60 μm | ASTM D3451 |
| Bulk density of powder | 0.425 g/cm^3 0.015 lb/in^3 | ASTM D1895 |

2.2 Sample Preparation

Samples were produced using an MJF experimental printer platform using voxels of with dimensions 23.6 μm by 23.6 μm by 100 μm . This printer is outfitted with multi-agent printing capability, which includes a combination of the functional agents: near infrared absorbing dye (NIRD), fusing agent, detailing agent, silver conductive agent, NaCl salt agent, cyan agent, yellow agent, magenta agent, and black agent. The printer is also outfitted with IR warming lamps, 650W tungsten halogen (QTH) IR fusing lamps, print bed, powder supply, and counter rotating powder spreader.

2.3 Measurement Methods

The thermal camera used was an FLIR A655sc with 25° lens. ResearchIR Max software is used for controlling the camera and collecting temperature profile data. The emissivity value was set to 0.95 [11][12].

The weights of 1.15 cm colored cube samples were measured using a Mettler Toledo XS205 Dual Range Balance.

3. Results and Discussion

Finding a thermally stable single printing parameter for specific parts to control heating is difficult and time consuming. By modulating agent loadings at the voxel level, the thermals can be controlled precisely and a uniform or controlled non-uniform fused part can be produced. However, the relationship between agent loading and heating is complicated by the fact that there are two competing thermal actors in a single agent. The liquid portion of the agent formulations cool the printed area while active IR absorbing components convert photo-energy into thermal energy to raise temperature for fusing plastic particles together. For

example, when IR fusing agent weight percentage is increased, correspondingly a higher heating effect is achieved. However, if it is increased to a greater extent, cooling effects will become dominant. Figure 1 shows this relationship, with higher density as an indicator of higher temperatures and longer sintering times reached, which result in increased elongation at break mechanical properties [13][14]. These two different outcomes from increasing fusing agent loading must be accounted for when controlling agent placement in combination with other functional agents loaded into a single voxel.

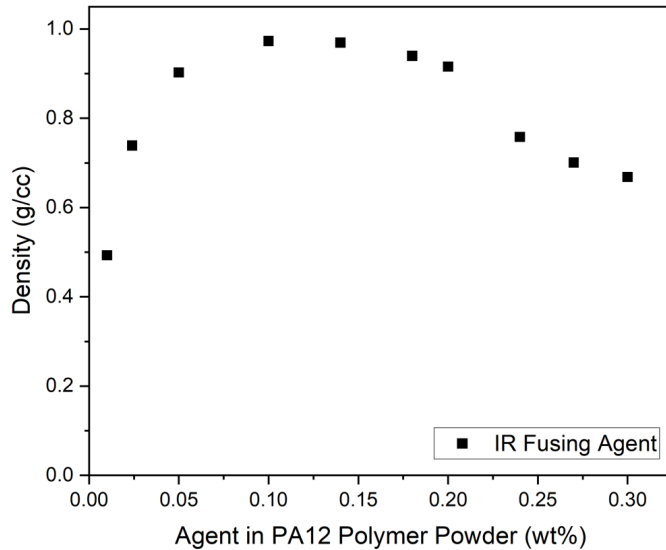


Figure 1. Fusing ability response to different weight percentage loadings of IR fusing agent in PA12 polymer powder.

Addressing these difficulties of printing with multiple IR absorption agents in a single part demands a need for a solution with accurate thermal control to define fusing capability with all colors or other functional agents throughout a part (conductive, mechanical etc.).

We have developed a new method of balancing fusing ability at the voxel level as shown by our work with color agents, each of which has a different thermal impact due to different IR energy absorbing and transmission to heat characteristics. The UV-Vis spectra shown in figure 2 is a strong indicator for IR energy absorption from the different agents and it was observed that the NIRD fusing agent has a well-matched absorption profile with the QTH lamp emitter. Also shown is the overlap or lack thereof for the colorant agents with cyan having the most absorption and yellow the least in the QTH emitting spectrum. However, it is important to note that the UV-Vis does not include the transmission of absorbed energy into heat. Therefore, observation utilizing a thermal camera of agent loading is essential to understanding the thermal impact performance.

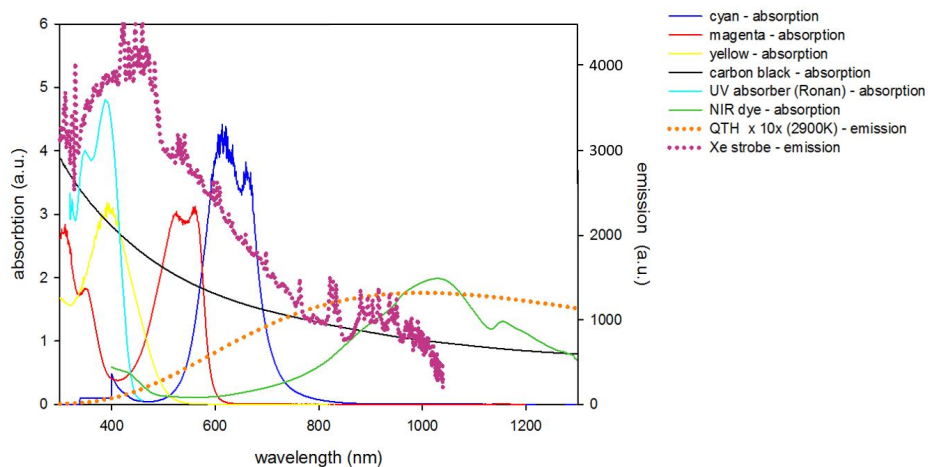


Figure 2. UV-Vis absorption spectrum for different dyes used in agent formulations.

We utilized a temperature profile of a part layer to determine fusing consistency throughout the part during the printing process to create a new agent placement for uniform fusing. This method can be used to answer questions like how to process a 3D printed part and how to generate files with agent loadings that balance both cooling and heating effects to manage thermal uniformity and build a mechanically uniform multi-colored part. By learning initial thermal behavior of each agent during the printing process on the same build bed generated by forward looking infrared radiometer (FLIR), we can capture the exact thermal differences between different agent loadings and fusing condition pairings on the powder bed. Therefore, we can digitally control the agent loading to “flatten” the temperature profile and ensure uniform fusing throughout multi-agent printed parts.

A base line fusing condition and agent placement file is generated for a set of 8 different colored 1.15 cm side length cubes utilizing this approach with uniform agent loading. During the printing process, the variation in temperature throughout the part is recorded. The base line fusing condition and agent placement temperature profile for 8 different colored cubes is shown in figure 3 with the corresponding agent loadings for this set of parts shown in table 2.

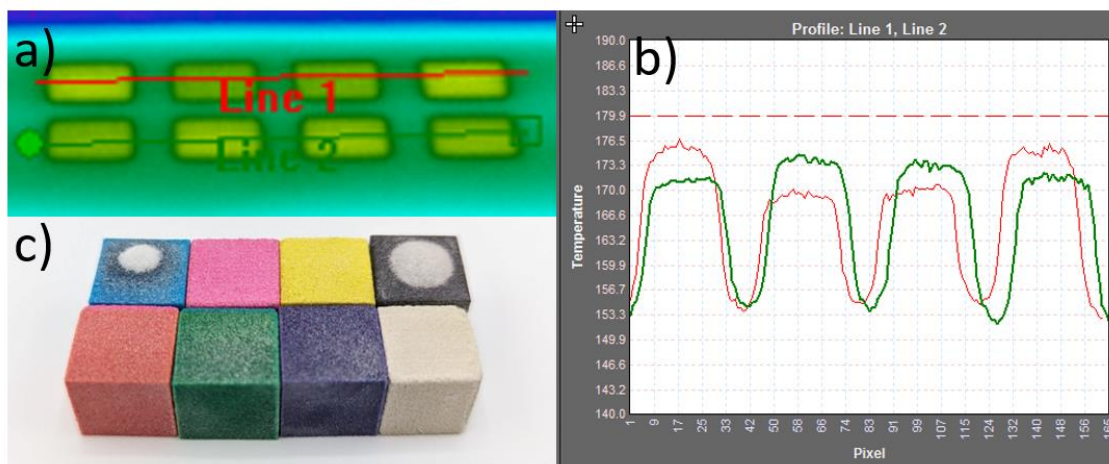


Figure 3. FLIR temperature profile data for 8 different colored cubes using a baseline agent

placement file with constant total agent loading per voxel a) FLIR image, b) temperature profile, and c) printed parts.

Table 2. Base line fusing condition agent placement with constant total agent loading.

| Agents | Cyan | Magenta | Yellow | NIRD | Black | Total |
|--------------------|-------|---------|--------|-------|-------|-------|
| Black Cube [wt%] | 0.020 | 0.016 | 0.016 | 0 | 0.105 | 0.157 |
| Blue Cube [wt%] | 0.026 | 0.026 | 0 | 0.105 | 0 | 0.157 |
| Green Cube [wt%] | 0.026 | 0 | 0.026 | 0.105 | 0 | 0.157 |
| Red Cube [wt%] | 0 | 0.026 | 0.026 | 0.105 | 0 | 0.157 |
| White Cube [wt%] | 0 | 0 | 0 | 0.105 | 0 | 0.105 |
| Yellow Cube [wt%] | 0 | 0 | 0.051 | 0.105 | 0 | 0.156 |
| Magenta Cube [wt%] | 0 | 0.051 | 0 | 0.105 | 0 | 0.156 |
| Cyan Cube [wt%] | 0.051 | 0 | 0 | 0.105 | 0 | 0.156 |

The magenta, yellow, and white cubes were under fused, below 90% density, so more NIRD FA was added to these color cubes. The black cube was over fused, so more colorant was added to cause cooling. The cyan cube was also over fused, but instead of increasing the colorant, which would have significantly altered the color, cyan agent was decreased due to cyan colorant’s high IR energy absorption and thermal energy transmittance properties. The corrected agent placement temperature profile is shown in figure 4 and the corresponding agent loading for producing this “flattened” temperature profile is shown in table 3.

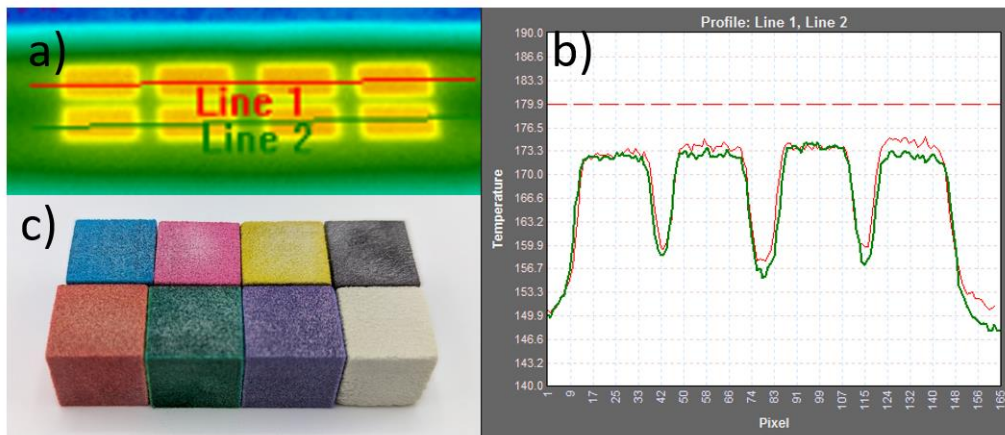


Figure 4. FLIR temperature profile data for 8 different colored cubes using the new balanced agent placement file a) FLIR image, b) temperature profile, and c) printed parts.

Table 3. Corrected printing profile agent placement using new method.

| Agents | Cyan | Magenta | Yellow | NIRD | Black | Total |
|--------------------|-------|---------|--------|-------|-------|-------|
| Black Cube [wt%] | 0.045 | 0.045 | 0.045 | 0 | 0.105 | 0.240 |
| Blue Cube [wt%] | 0.026 | 0.026 | 0 | 0.105 | 0 | 0.157 |
| Green Cube [wt%] | 0.026 | 0 | 0.026 | 0.105 | 0 | 0.157 |
| Red Cube [wt%] | 0 | 0.026 | 0.026 | 0.111 | 0 | 0.163 |
| White Cube [wt%] | 0 | 0 | 0 | 0.111 | 0 | 0.111 |
| Yellow Cube [wt%] | 0 | 0 | 0.051 | 0.111 | 0 | 0.162 |
| Magenta Cube [wt%] | 0 | 0.048 | 0 | 0.111 | 0 | 0.159 |
| Cyan Cube [wt%] | 0.048 | 0 | 0 | 0.105 | 0 | 0.159 |

When the thermal history is similar with same geometry and printing orientation, similar mechanical properties are achieved for printed parts [15]. We achieve this similar thermal history by creating a flat thermal profile as measured by the FLIR. Table 4 shows the 8 colored cubes and their uniform weight measurements affiliated with the uniform fusing conditions indicated by the temperature profile chart shown in Figure 4. Notice that the white cube was still under fused and still needs a slight increase of NIRD fusing agent to achieve better fusing.

Table 4. Different colored 1.15 cm side length cube weights comparison between uniform agent loading and corrected agent loading prints.

| Color cube | C | M | Y | K | R | G | B | W |
|---|------|------|------|------|------|------|------|------|
| Uniform agent loading part weight [g] | 1.54 | 1.25 | 1.31 | 1.67 | 1.40 | 1.52 | 1.47 | 1.15 |
| Corrected agent loading part weight [g] | 1.53 | 1.50 | 1.48 | 1.59 | 1.43 | 1.47 | 1.49 | 1.24 |

Another example of a multi-functional MJF part is the smart link. This part comprises of a nylon link containing an imbedded silver conductive nylon polymer and silver composite strain gauge. To process this part, the conductive voxels need a lower temperature maintained in the silver trace as compared to the bulk nylon of the rest of the link to ensure the silver trace is intact without isolated segments from non-conductive polymer flow. To achieve this, variable fusing ability control must be utilized. Fusing is balanced to ensure agent in the conductive trace creates a lower fusing ability than the rest of the link by increasing DA and decreasing FA loading in the conductive voxels. Parts printed with this technique are shown in figure 5. The original agent loading for the part that produced non-conductive traces compared to the agent loading for producing a strong mechanical chain link with conductive traces are shown in table 5.

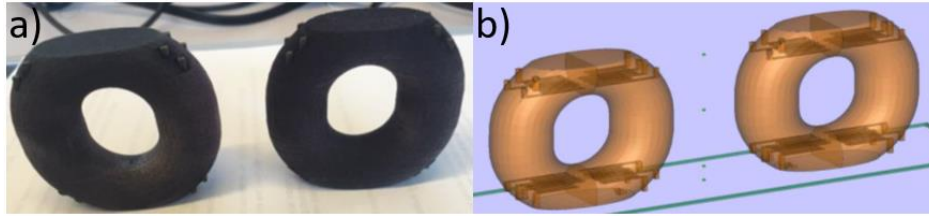


Figure 5. Conductive traces in smart link embedded strain gauge a) 3D printed parts and b) CAD model.

Table 5. Agent placement weight percentages used for non-conductive chain link part compared to conductive traces.

| Agent | NaCl | Silver | FA | DA |
|----------------------------|-------|--------|-------|-------|
| Non-conductive trace [wt%] | 0.299 | 0.897 | 0.051 | 0.061 |
| Non-conductive link [wt%] | 0 | 0 | 0.051 | 0.061 |
| Conductive trace [wt%] | 0.299 | 0.897 | 0.013 | 0.151 |
| Conductive link [wt%] | 0 | 0 | 0.013 | 0.151 |

FA – fusing agent
 DA – detailing agent
 NaCl – salt agent
 Silver – silver conductive agent

The method described is used to create agent loading profiles for multi-colored and imbedded conductive trace parts as shown in figure 6.

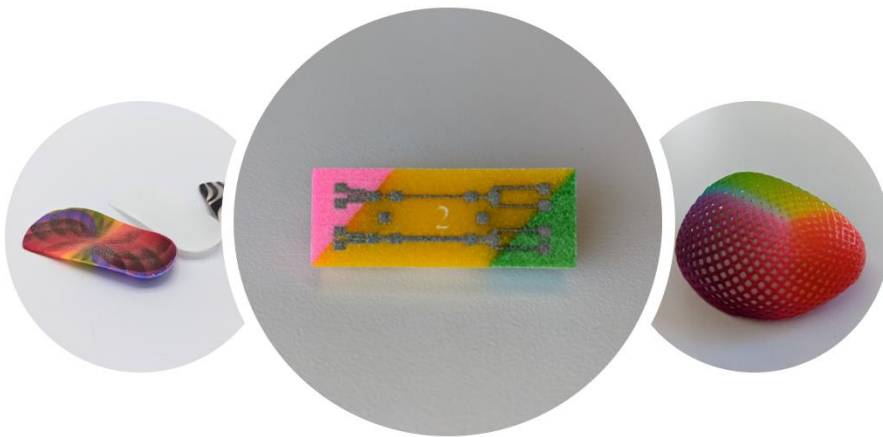


Figure 6. Multi-functional MJF printed parts including both multi-color and conductive traces.

4. Conclusion

A method for producing both non-uniformly fused imbedded conductive traces and multi-colored uniform fused parts is achieved by characterizing the absorption and thermal conversion of different functional agents. FLIR temperature profile monitoring and part functionality (conductivity or part weight) are used to quantify performance. This agent

balancing method for controlling the temperature of functional voxels printed with multi-functional agents is needed to realize the MJF and produce single parts with varying voxel properties. A patent has been granted covering this method and is utilized in developing print processes for new functional agents [16].

5. Acknowledgements

This work was funded by HP Laboratories. We thank Yan Zhao, for early collaborative development on this subject. The authors gratefully acknowledge the support of the HP 3D business extended 3D print team.

6. References

- [1] Schwab, Klaus. (2023). The Fourth Industrial Revolution. *Britannica*. <https://www.britannica.com/topic/The-Fourth-Industrial-Revolution-2119734>
- [2] Dilberoglu, U. M, Gharehpapagh B., Yman, U., & Dolen, M. (2017). The Role of Additive Manufacturing in the Era of Industry 4.0. *Procedia Manufacturing*, vol. 11, pp. 545–554. <https://doi.org/10.1016/j.promfg.2017.07.148>
- [3] Rosso, S., Meneghello, R., Biasetto, L., Grigolato, L. Concheri, G., & Savio, G. (2020). In-Depth Comparison of Polyamide 12 Parts Manufactured by Multi Jet Fusion and Selective Laser Sintering. *Additive Manufacturing*, vol. 36. <https://doi.org/10.1016/j.addma.2020.101713>
- [4] Wohlers, T. T. (2019). Wohlers Report 2019: 3D Printing and Additive Manufacturing State of the Industry. *Wohlers Associates*.
- [5] Zhu, Z., & Majewski, C. (2020). Understanding pore formation and the effect on mechanical properties of High Speed Sintered polyamide-12 parts: A focus on energy input. *Materials & Design*, vol. 194. <https://doi.org/10.1016/j.matdes.2020.108937>
- [6] Wittkopf, J.A., Erickson, K., Olubummo, P., Hartman, A., Tom, H., & Zhao, L., (2019) 3D Printed Electronics with Multi Jet Fusion. *Society for Imaging Science and Technology*. <https://doi.org/10.2352/ISSN.2169-4451.2019.35.29>
- [7] Erickson, K. J., Hartman, A., Zhao, L., Tom, H. S., Zhao, Y., & Fitzhugh, A. (2020). *Three-dimensional (3D) printing*. (US Patent No. 10,647,053). <https://image-ppubs.uspto.gov/dirsearch-public/print/downloadPdf/10647053>
- [8] Olubummo, A., Hartman, A., Wycoff, K., & Zhao, L., (2022). *Three-dimensional printing*. (US Patent No. 11,383,435). <https://image-ppubs.uspto.gov/dirsearch-public/print/downloadPdf/11383435>
- [9] HP Official Site. (2018). HP Jet Fusion 580 Color 3D Printer – Manuals. <https://support.hp.com/us-en/product/hp-jet-fusion-500-3d-printer-series/21430573/model/21430578/manuals>
- [10] HP Official Site. (2020). HP 3D Printing Materials for HP Jet Fusion 5200/4200 Series 3D Printing Solutions. <https://h20195.www2.hp.com/v2/getpdf.aspx/4AA7-1533ENA.pdf>

- [11] Diller, T., Sreenivasan, R., Beaman, J., Bourell, D., & LaRocco, J., (2010). Thermal Model of the Build Environment for Polyamide Powder Selective Laser Sintering. *Solid Freeform Fabrication Symposium*.
<https://repositories.lib.utexas.edu/bitstream/handle/2152/88277/2010-45-Diller.pdf?sequence=2>
- [12] Chen, J., Tan, P., Liu, X., Tey, W., Ong, A., Zhao, L., & Zho, K., (2022). High-strength light-weight aramid fibre/polyamide 12 composites printed by Multi Jet Fusion. *Virtual and Physical Prototyping*, 17:2, 295-307. <https://doi.org/10.1080/17452759.2022.2036931>
- [13] Ellis, A., Noble C., & Hopkinson, N., (2014). High Speed Sintering: Assessing the influence of print density on microstructure and mechanical properties of nylon parts. *Additive Manufacturing*, 1-4, 48-51. <https://doi.org/10.1016/j.addma.2014.07.003>
- [14] Nussbaum, J., Kaur, T., Harmon, J., & Crane, N., (2021). Impact of sintering time and temperature on mechanical properties in projection sintering of Polyamide-12. *Additive Manufacturing*, 37, 101652. <https://doi.org/10.1016/j.addma.2020.101652>
- [15] Kiani, A., Khazaei, S., Badrossmary, M., Foroozmehr, E., & Karevan M., (2020). An Investigation into Thermal History and Its Correlation with Mechanical Properties of PA12 Parts Produced by Selective Laser Sintering Process. *Journal of Materials Engineering and Performance*, 29, 832-840. <https://doi.org/10.1007/s11665-020-04640-0>
- [16] Hartman, A., Olubummo, P., Erickson K. J., Zhao, L., & Tom. H. S., (2022). *Temperature control in 3D object formation*. (US Patent No. 11,511,479). <https://image-ppubs.uspto.gov/dirsearch-public/print/downloadPdf/11511479>